

Coherent Structures in the Axisymmetric Turbulent Jet Mixing Layer

Mark N. Glauser, Stewart J. Leib, William K. George

Department of Mechanical and Aerospace Engineering, State University of New York at Buffalo, Buffalo, New York 14260, USA

Abstract

In 1967 Lumley proposed two different, but complimentary approaches to the objective determination of coherent structures. The first uses an orthogonal decomposition to extract eigenvectors from two point velocity measurements, the lowest order eigenvector representing the largest structure. Where there are partial homogeneities, or when the flow is stationary, the eigenfunctions are the harmonic ones and the coherent features are impossible to identify. To organize these fluctuating Fourier modes into coherent features, a second decomposition is used, the shot-noise decomposition.

The initial experiment (on which this paper is based) has generated cross-spectral data at seven radial positions across the jet mixing layer. The 49 cross-spectra have then been decomposed to obtain the eigenvectors and the time development of the streamwise velocity component of the large eddies in the mixing layer. The results to date show clearly the existence of a large scale structure in the mixing layer containing 40% of the turbulent energy. The second and third order structures contain another 40% of the energy. Thus nearly all the energy is contained in the first three modes.

Nomenclature

$a_{(n)}$	Random coefficients	x	Special vector
f	Characteristic eddy	y	Radial distance across jet mixing layer
g	Random distribution function	α	Inner product of velocity vector and candidate eddy
R_{ij}	Velocity correlation tensor	δ_{mn}	Kroneker delta function
S	Streamwise velocity spectrum	$\lambda^{(n)}$	Eigenvalues
t	Time	Φ_{ij}	Cross spectral tensor
u	Velocity vector	ϕ	Eigenvectors
u	Streamwise velocity	ψ	Eigenvectors in transformed domain
\hat{u}	Fourier transform of velocity	ω	Frequency
W	Weighting function		

Introduction

The earliest investigations of the statistical characteristics of the turbulence in an axisymmetric jet mixing layer were carried out by Laurence (1956), Davies et al. (1963), and Bradshaw et al. (1964). Qualitative models for the large scale structures in a number of turbulent flows were formulated by Grant (1958) and Townsend (1956, 1976). Crow and Champagne (1971) found identifiable structures in a jet which resembled large scale vortical puffs.

Recently it has been found that these eddies may be more orderly and energetic than was first imagined. Also experiments indicate that these eddies are coherent in some sense. That is, they travel downstream as an identifiable entity for some distance before mean shear distortion and energy exchange with smaller scales destroy them.

While the precise role of the eddies in the dynamics of the flow is not yet established, they are suspected of being responsible for the entrainment process in addition to acting as

sources of noise. For a review of some of the more recent work on coherent structures see Cantwell (1981).

Lumley (1967) has proposed two different, but complimentary approaches to the objective determination of coherent structures, the orthogonal decomposition for inhomogeneous directions and the shot noise decomposition for homogeneous directions and for time if the process is stationary. These two approaches are implemented in this paper.

In the current work, experiments were carried out in the mixing region of an axisymmetric turbulent jet to acquire the necessary data to perform a one-dimensional shot noise decomposition and a scalar two-dimensional version of the full orthogonal decomposition. Numerical computations were carried out and the eigenfunction and characteristic eddies were extracted from these measurements. The power spectra as well as the instantaneous velocity signals were reconstructed from these eigenfunctions.

Experiment and Apparatus

Briefly, the experiment was performed in a circular air jet facility. The jet nozzle was of fifth order polynomial design and has an exit diameter of 0.098 m with a contraction ratio of 10:1. The exit conditions of the jet are as follows: The turbulence intensity was 0.35%, the Reynolds number was 110,000 and the boundary layer thickness at the exit ($u = 0.99 u_e$) was 0.0012 m. A specially-designed probe containing seven single hot wire sensors positioned at $x/d = 3$ was used to carry out the experiment. The individual sensors were spaced 0.0127 m apart with the center sensor in the middle of the mixing layer. Leib et al. (1984) provide a more complete description of the experiment.

The Orthogonal Decomposition

In 1967 Lumley proposed that the coherent structure should be that structure which has the largest mean square projection on the velocity field. If $\phi(x, t)$ is our candidate structure, then we should choose ϕ to maximize

$$\overline{|\mathbf{u} \cdot \phi|^2} = \overline{|\alpha|^2}, \quad (1)$$

where $\mathbf{u} = \mathbf{u}(x, t)$ is the instantaneous velocity. ϕ is then, in some sense at least, the most likely occurrence of \mathbf{u} . The quantity in (1) is assumed normalized by the amplitude of the candidate structure so that the projection is only affected by the shape of the candidate and not by its amplitude.

Maximizing $\overline{|\mathbf{u} \cdot \phi|^2}$ leads to the following eigenvalue problem:

$$\iiint R_{ij}(\mathbf{x}, \mathbf{x}', t, t') \phi_j(\mathbf{x}', t') d\mathbf{x}' dt' = \lambda^{(n)} \phi_i(\mathbf{x}, t), \quad (2)$$

where $R_{ij}(\mathbf{x}, \mathbf{x}', t, t') = \overline{u_i(\mathbf{x}, t) u_j(\mathbf{x}', t')}$ and $\lambda = |\alpha|^2$.

Equation (2) has an infinity of orthogonal solutions and the original random field can be reconstructed from them, i.e.,

$$\mathbf{u}(\mathbf{x}, t) = \sum_{n=1}^{\infty} a_n \phi^{(n)}(\mathbf{x}, t). \quad (3)$$

The a 's are random and uncorrelated, i.e.,

$$\overline{a_n a_m} = \lambda_n \delta_{mn},$$

where the λ_n are the eigenvalues.

If there are stationarities or homogeneities these must first be removed by Fourier analysis, that is,

$$u(\mathbf{x}, t) \rightarrow \hat{u}(\mathbf{x}, \omega).$$

Now decompose \hat{u} to get

$$\int \Phi_{ij}(\mathbf{x}, \mathbf{x}', \omega) \psi_j(\mathbf{x}', \omega) d\mathbf{x}' = \lambda^{(n)}(\omega) \psi_i(\mathbf{x}, \omega), \quad (4)$$

where the integral is over inhomogeneous directions and $\Phi_{ij}(\mathbf{x}, \mathbf{x}', \omega)$ is the cross spectral tensor.

The eigenvalues now become eigenspectra

$$\lambda^{(n)} \rightarrow \lambda^{(n)}(\omega)$$

and the eigenvectors are frequency dependent,

$$\phi_i^{(n)}(\mathbf{x}, t) \rightarrow \psi_i^{(n)}(\mathbf{x}, \omega).$$

The Fourier transform of the velocity can be reconstructed as

$$\hat{u}(\mathbf{x}, \omega) = \sum_{n=1}^{\infty} a_n(\omega) \Psi^{(n)}(\mathbf{x}, \omega), \quad (5)$$

where the a 's are random and uncorrelated functions of frequency, i.e., $\overline{|a_n(\omega)|^2} = \lambda^{(n)}(\omega)$, and can be obtained for a single ensemble by

$$a_n(\omega) = \int \hat{u}(\mathbf{x}, \omega) \Psi^{(n)*}(\mathbf{x}, \omega) d\mathbf{x}.$$

Note that $\hat{u}(\mathbf{x}, \omega)$ and $a_n(\omega)$ are random and $\lambda^{(n)}(\omega)$ and $\psi^{(n)}(\mathbf{x}, \omega)$ are deterministic.

The spectrum can also be reconstructed at each position by

$$S(\mathbf{x}, \omega) = \sum_{n=1}^{\infty} \lambda^{(n)}(\omega) |\psi^{(n)}(\mathbf{x}, \omega)|^2 \quad (6)$$

as can the cross-spectra

$$\Phi_{ij}(\mathbf{x}, \mathbf{x}', \omega) = \sum_{n=1}^{\infty} \lambda^{(n)}(\omega) \psi_i^{(n)}(\mathbf{x}, \omega) \psi_j^{(n)*}(\mathbf{x}', \omega). \quad (7)$$

A Simpler Version

A scalar, one-dimensional version of the orthogonal decomposition, which utilizes the one-dimensional cross-spectra measured in the jet can be derived and formulated as

$$\int \Phi_{11}(y, y', \omega) \psi^{(n)}(y', \omega) dy' = \lambda^{(n)}(\omega) \psi^{(n)}(y, \omega), \quad (8)$$

where y is the radius in the mixing layer. The Fourier transform of the streamwise velocity can be reconstructed by

$$\hat{u}(y, \omega) = \sum_{n=1}^{\infty} a_n(\omega) \psi^{(n)}(\omega, r), \quad (9)$$

where

$$a_n(\omega) = \int \hat{u}(y, \omega) \psi^{(n)*}(y, \omega) dy.$$

The spectrum is reconstructed from

$$S(y, \omega) = \sum_{n=1}^{\infty} \lambda^{(n)}(\omega) |\psi^{(n)}(y, \omega)|^2, \quad (10)$$

where λ_n are the eigenspectra.

Using the measured values of the cross spectrum, (8) can be solved numerically for the eigenvalues and eigenfunctions.

The Numerical Approximation

Briefly, the numerical approximation consists basically of replacing the integral in (8) by a suitably chosen quadrature rule. This can be written in general as

$$\sum_{i=1}^m W(y_i) \Phi(y_j, y_i, \omega) \psi^{(n)}(y_i, \omega) = \lambda^{(n)}(\omega) \psi^{(n)}(y_j, \omega), \quad (11)$$

$$j = 1, 2, \dots, m,$$

where m is the maximum number of radial locations and $W(y_i)$ is a weighting function. In the present case $m = 7$. Equation (11) is now an algebraic eigenvalue problem.

Now the matrix formed from the values of Φ is complex Hermitian. That is

$$\Phi_{ij} = \Phi_{ji}^*. \quad (12)$$

However, the weighted matrix formed by $W(y_i) \Phi(y_j, y_i)$ no longer has this property. It is desirable, in the numerical solution of eigenvalue problems, to keep the coefficient matrix Hermitian (Baker, 1977).

Operating on both sides of (11) by $W(y_j)^{1/2}$ results in the following eigenvalue problem,

$$\sum_{i=1}^m [W^{1/2}(y_j) \Phi(y_j, y_i, \omega) W^{1/2}(y_i)] W^{1/2}(y_i) \psi^{(n)}(y_i, \omega) = \lambda^{(n)}(\omega) W^{1/2}(y_j) \psi^{(n)}(y_j, \omega), \quad (13)$$

where now the matrix $W(y_j)^{1/2} \Phi(y_j, y_i, \omega) W(y_i)^{1/2}$ is Hermitian. Since this matrix is similar to that in (11), they have the same eigenvalues. The original eigenvectors can be recovered from those obtained from (13) by operating by $W(y_j)^{-1/2}$, i.e.

$$\psi^n(y_j, \omega) = W(y_j)^{1/2} \psi^n(y_j, \omega) W(y_j)^{-1/2}.$$

Simpson's one-third rule was chosen as the quadrature rule for its accuracy and simplicity. For a more detailed discussion of the numerical approximation see Leib et al. (1984).

Results of the Orthogonal Decomposition Analysis

The results show clearly the existence of a large structure in the mixing layer containing 40% of the turbulent energy. The second and third order structures contain together another 40% of the energy, the remainder being contained in structures impossible to resolve because of statistical and numerical errors.

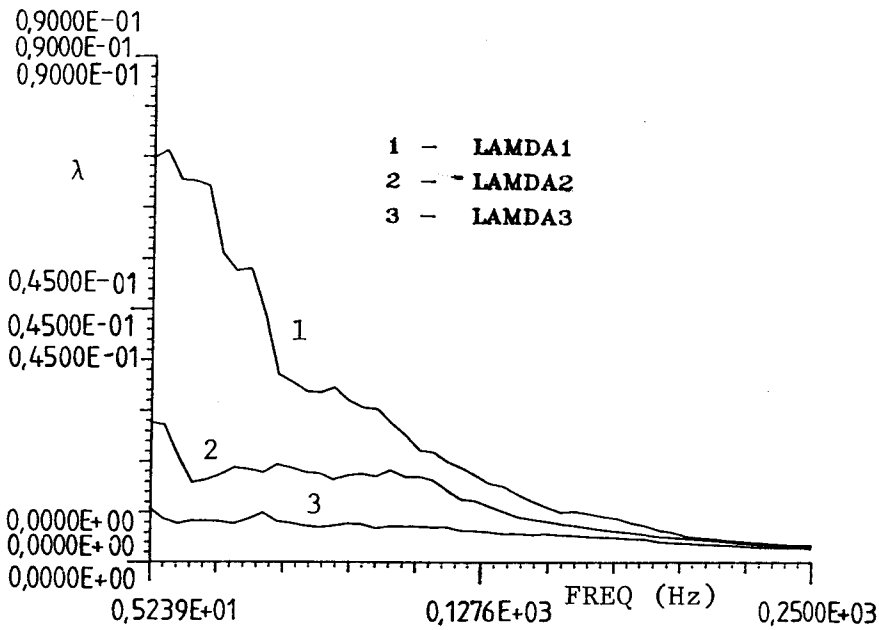


Fig. 1. Eigenspectra showing how energy is distributed among the first three eigenvalues

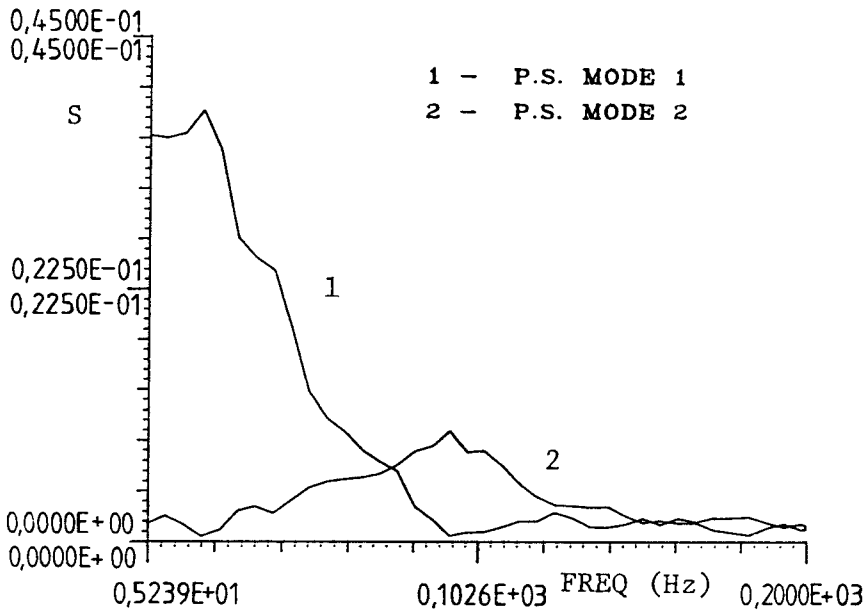


Fig. 2. Individual contributions to the power spectrum from first 2 modes

Figure 1 shows the eigenspectra for the three dominant modes. These eigenvalues represent the contribution to the total energy (integrated across the shear layer) from the various modes. It was found that the first mode contained about 40% of the total energy.

As was shown earlier (10), the power spectra at each radial position can be expanded in a series of the eigenmodes since each mode makes an independent contribution to the spectrum. Figure 2 shows the contributions from the first two modes to the power spectrum at a position on the low speed side of the mixing layer. It can be seen from this figure that the contribution to the power spectrum from the first mode peaks at very low frequency, while that of the second peaks at a higher frequency. This was found to be the case at the

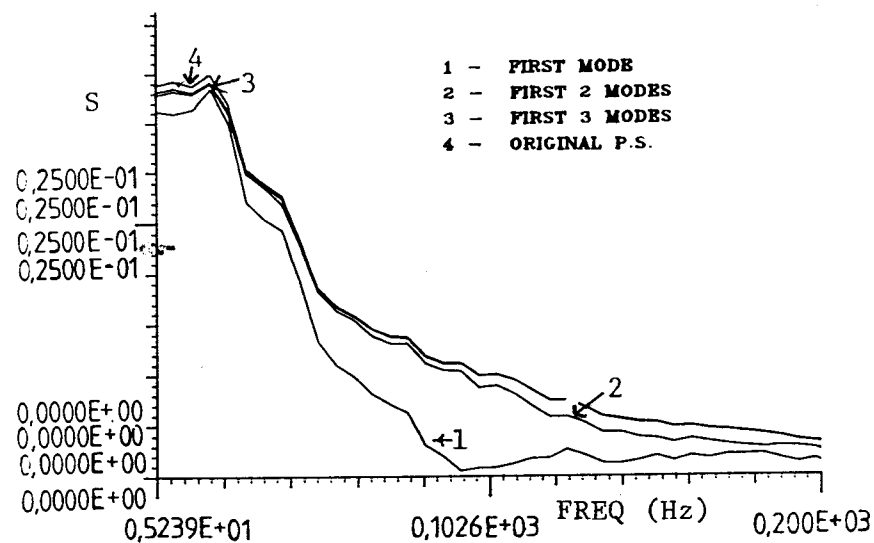


Fig. 3. Convergence of power spectrum

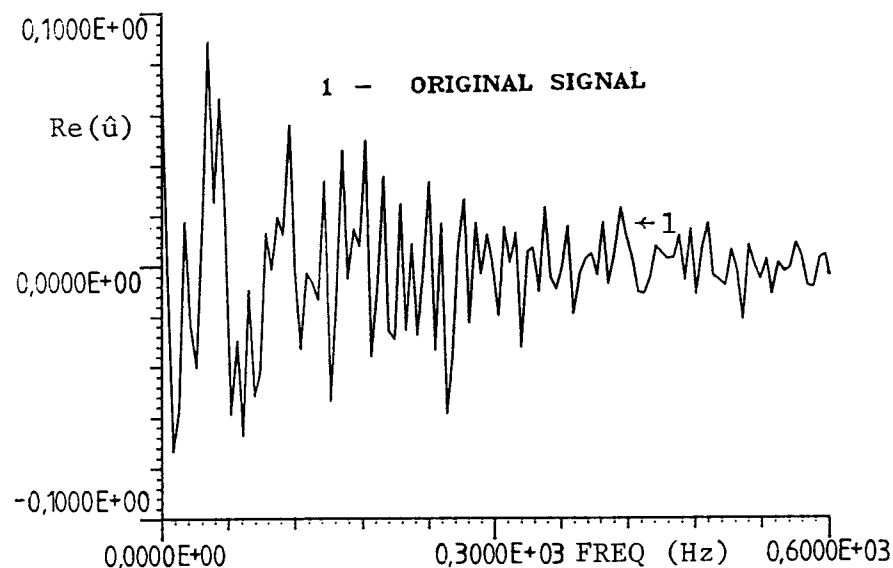


Fig. 4. Real part of F.T. of original signal

other radial positions as well. In this sense then, we see that the dominant mode is indeed representative of the larger scales in the flow.

Figure 3 [using (10) for $n = 1, 2, 3$] shows the convergence of the expansion for this power spectrum. Similar results were obtained at the other locations. These results show that nearly all the energy is contained in the first three modes.

From the spectral data it might be expected that the instantaneous velocity signal could be represented adequately with these three modes. After application of (9) this is indeed seen to be the case (see Figs. 4–7). Figure 4 is one record of the original velocity signal in the center of the mixing layer (real part of its Fourier transform). Figure 5 shows the super-

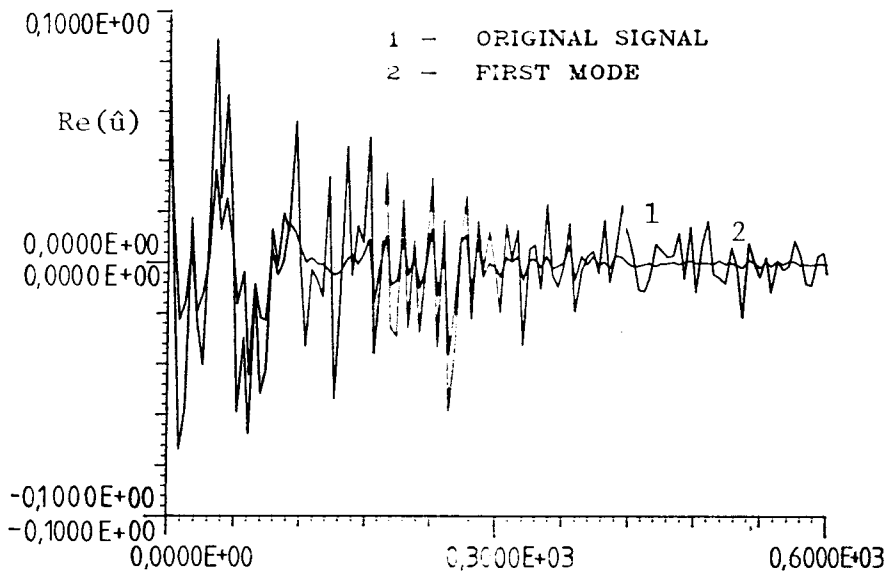


Fig. 5. First mode superimposed on original

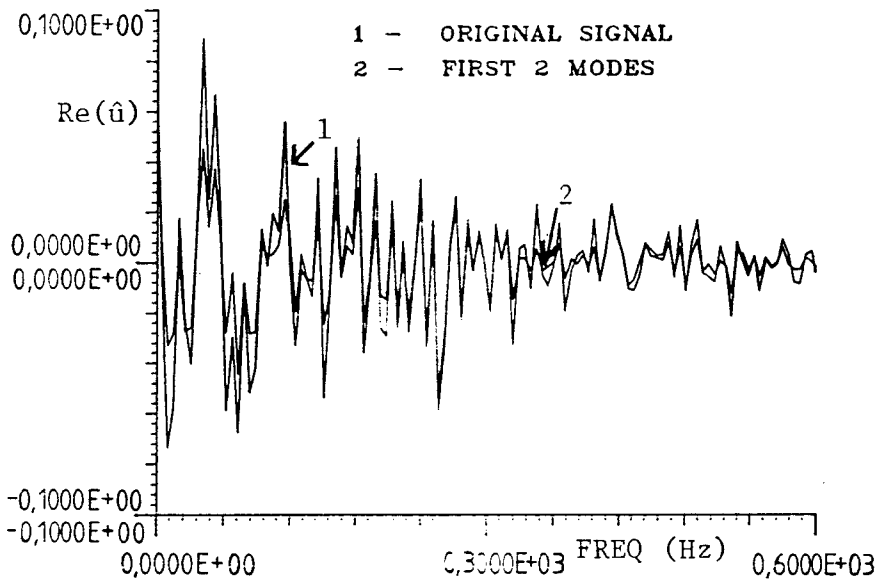


Fig. 6. First 2 modes superimposed on original

position of the 1st mode [$n = 1$ in (9)] on the original signal. Figure 6 shows the first 2 modes. Figure 7 shows the first 3 modes. As can be seen from Fig. 7, almost the entire signal has been reconstructed from the summation of the first 3 modes.

The question may be asked, what do these eigenfunctions that maximize the mean square projection look like? The fact that the eigenvalue problem was solved as a function of radial position for each discrete frequency dictates that there is an individual set of eigenfunctions for each frequency. Since the eigenfunctions are functions of frequency and radial position in the jet mixing layer it is of interest to look at the surfaces generated by them. However these surfaces have been found to be quite complex. Because of this, different cross-sections were examined. The real and imaginary parts of the first three eigenfunctions at a frequency of 5.2 Hz are shown, plotted as a function of radial distance in the jet mixing layer, in Figs. 8

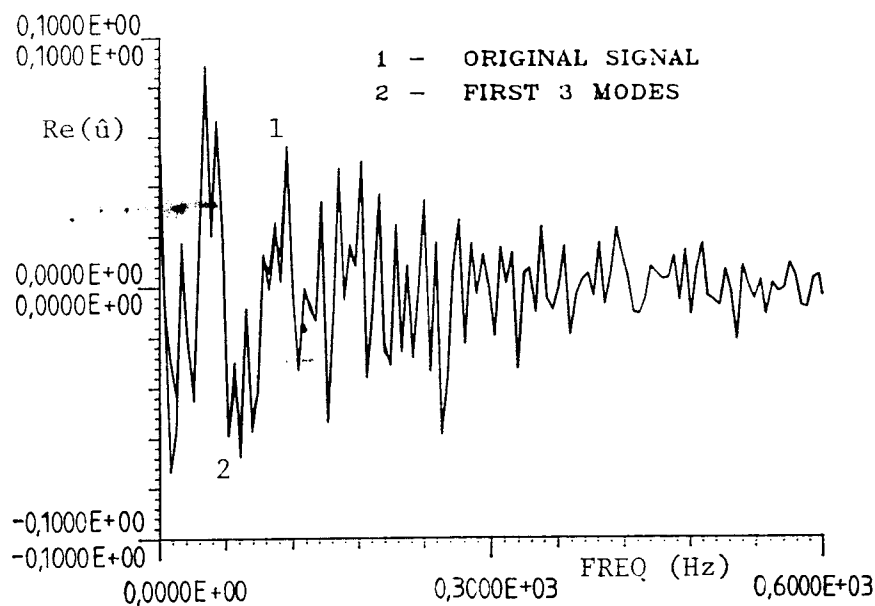


Fig. 7. First 3 modes superimposed on original. Note: Essentially no difference

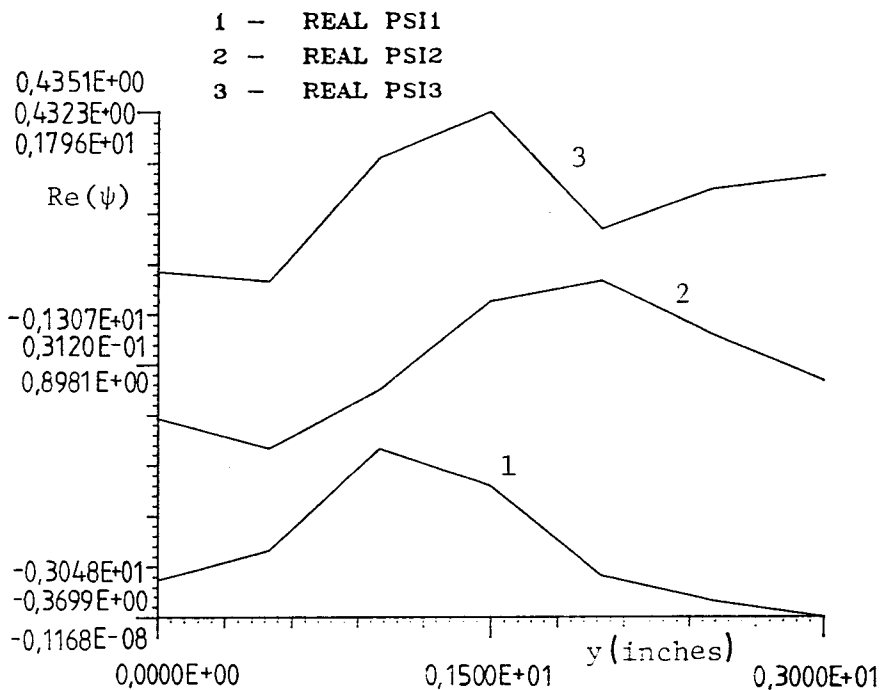


Fig. 8. Real parts of first 3 eigenfunctions at 5.2 Hz plotted as a function of radial distance in jet mixing layer

and 9 respectively. When examining these figures it appears that the first mode is symmetric and bears resemblance to the RMS plots across the jet mixing layer. The second mode is asymmetric and the third mode is even more complicated.

The real and imaginary part of the first eigenfunction for a radial position at the center of the mixing layer are plotted as a function of frequency in Fig. 10. This first eigenfunction eventually decays as the frequency approaches 1000 Hz. This was not the case for the second eigenfunction at the same radial position. Its real and imaginary parts are shown in Fig. 11.

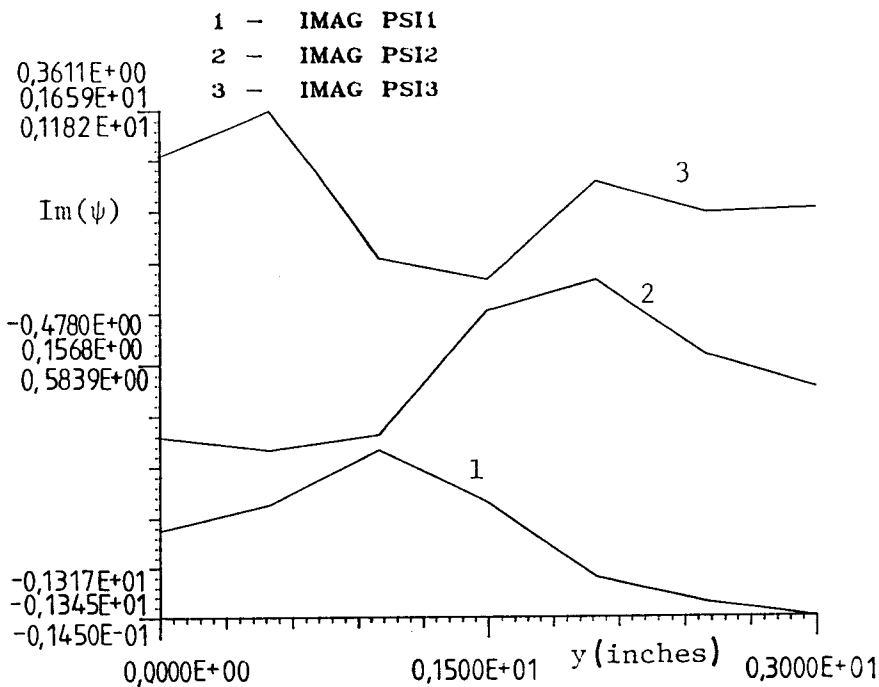


Fig. 9. Imaginary parts of first 3 eigenfunctions at 5.2 Hz plotted as a function of radial distance in the jet mixing layer

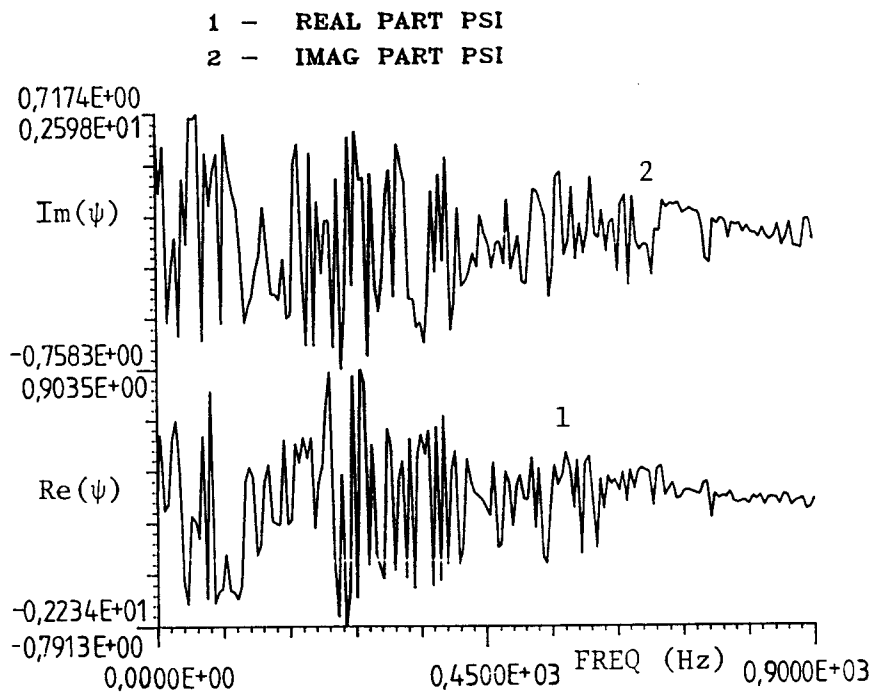


Fig. 10. Real and imaginary parts of first eigenfunction at the center of the mixing layer plotted as a function of frequency

When examining Fig. 11 one observes that the eigenfunction decays with frequency up to approximately 900 Hz but then starts to become large again. A plausible explanation for this observation is as follows. The smallest time scale for a typical eddy that can be resolved is dictated by the probe spacing and the appropriate convection velocity (since eddies smaller than this will not be seen by both probes). If it is assumed that the turbulence field is frozen

1 - REAL PSI2
2 - IMAG PSI2

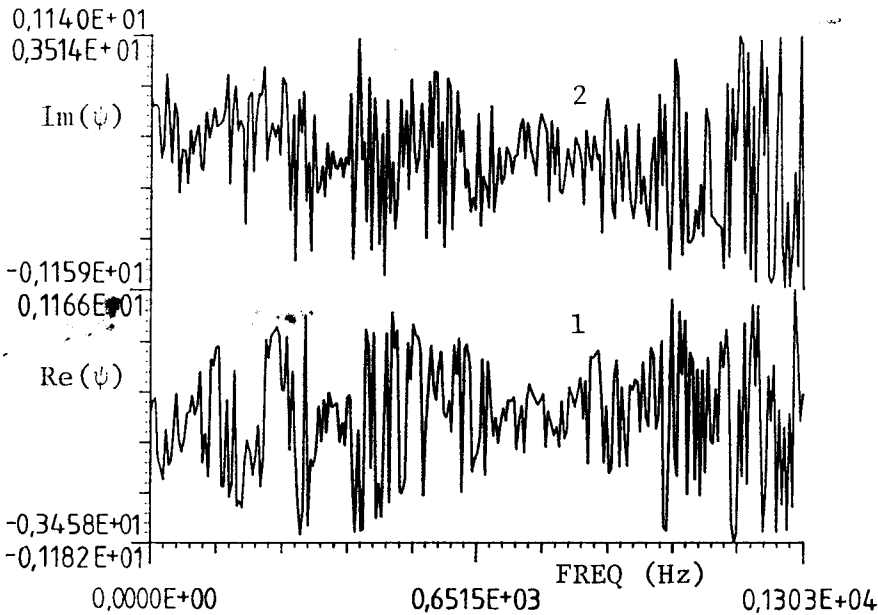


Fig. 11. Real and imaginary parts of 2nd eigenfunction at the center of the mixing layer plotted as a function of frequency

then this time scale is approximately equal to $\Delta y/u_c = 0.00115 \text{ sec} = \Delta t$. Now the resolvable bandwidth in frequency would approximately be equal to $1/\Delta t \cong 870 \text{ Hz}$. It is felt then that the results in Fig. 11 beyond 900 Hz are just a result of numerical noise.

The Shot Noise Decomposition

How is the coherent structure extracted from the analysis so far and in particular, what does the large eddy look like in physical space? This is difficult to answer. Remember that the coherent structure is defined to be the dominant mode, i.e.

$$\hat{u}^{(1)}(y, \omega) = a_{(1)}(\omega) \psi^{(1)}(y, \omega) \quad (14)$$

$$\text{or } u^{(1)}(y, t) = \int_{-\infty}^{\infty} e^{i\omega t} a_{(1)}(\omega) \psi^{(1)}(y, \omega) d\omega, \quad (15)$$

where because $a_1(\omega)$ is random, so is $\hat{u}^{(1)}$.

The visibility of the coherent structure depends on the bandwidth of the random coefficient $a_{(1)}(\omega)$. For low Reynolds number flow there are only a few Fourier coefficients so that the structure is visible, however with high Reynolds flow there are many Fourier coefficients resulting in the structure being invisible. Therefore a method is needed to organize these random pieces into 'groups'. This motivates the use of the shot noise decomposition.

The shot effect can be illustrated by the randomly varying intensity of a flow of electrons from cathode to anode in a vacuum tube. The signal produced by this stream of electrons is random in nature. The arrival of a single electron at the anode would result in a signal characteristic of this event. The signal which results from the arrival of many electrons at random times is then a random superposition of these characteristic signals. It can be seen then that, while the overall signal is indeed random, it is composed of characteristic signals

which are deterministic and occur at random times. The shot noise decomposition provides a means of determining the nature of the individual events from measurements of the spectrum of the random signal.

In extending these ideas to a homogeneous or stationary turbulent flow field it is supposed that the random velocity field is composed of characteristic signals or 'eddies', occurring at random times in a stationary flow (or at random positions in a homogeneous flow). Upon randomly superposing (or sprinkling the flow with) these eddies the random velocity field is realized.

These concepts were applied to the measurements of the streamwise velocity component as a function of the stationary variable time. In this case the shot noise decomposition, as suggested by Lumley, can be formulated as

$$u(t) = \int f(t - \tau) g(\tau) d\tau. \quad (16)$$

In (16), u is the streamwise velocity, (in our case, the velocity field of the large eddy $u^{(1)}$), f is the characteristic eddy, and g is a random function of time which serves to distribute the characteristic eddies. The function g is defined so that it is uncorrelated with itself. That is

$$\overline{g(t) g(t')} = \delta(t' - t). \quad (17)$$

The problem of determining the characteristic eddy then reduces to determining the function f . It is straightforward to show (Lumley, 1967) that this function is given by

$$f(y, t) = (1/2\pi)^{1/2} \int e^{-i\omega t} \sqrt{\frac{\lambda^{(1)}(\omega)}{2\pi}} |\psi^{(1)}(y, \omega)| d\omega. \quad (18)$$

It is important to note at this time that only the magnitude of the characteristic eddy can be recovered by (18), all phase information is lost. The phase can be recovered by examining the third-order statistics in a manner somewhat like that suggested by Lumley (1981). This will be discussed in a subsequent paper.

At each radial position (18) was used to construct the characteristic eddy using only its magnitudes (ie., ignoring possible phase differences across the mixing layer). The results of these computations are shown in Fig. 12. In this figure the form of the characteristic eddy as a function of time is shown for each radial position. A dominant peak occurred at a

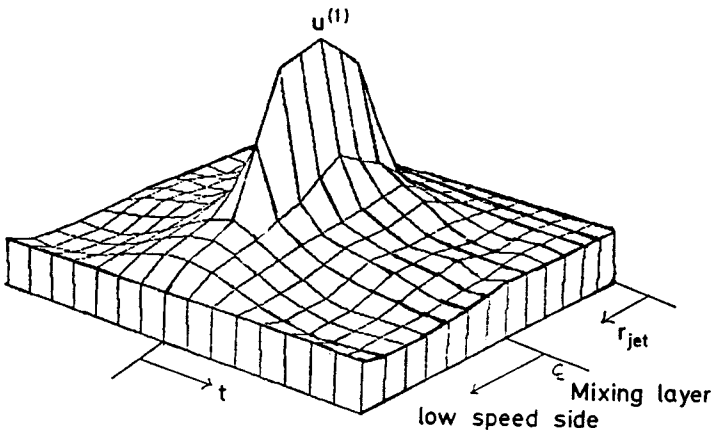


Fig. 12. Coherent structure calculated from Eq. (15)

position in the center of the mixing layer, as might have been expected. It is possible to argue from continuity and axisymmetry that this structure corresponds to a vortex ring-like structure not unlike that educted by Hussain (1981).

Conclusion

The orthogonal decomposition has been shown to be remarkably efficient at organizing data (i.e., 7×7 grid appears adequate) and the instantaneous properties of the random signal have not been lost, only organized. So efficient has the scheme been at organizing the energy that only a few terms were needed to completely represent the instantaneous signal.

The implications of these findings on the problem of turbulence modelling could be profound. If, in fact, the large scale features of turbulent flows can be resolved on such a coarse grid, a direct decomposition of the Navier-Stokes equation (Lumley, 1981) might represent a fruitful approach. The largest eddies would be calculated directly and the remainder of the turbulence modelled in more traditional ways.

It is difficult to determine the significance of the form of the coherent structures here due to the fluctuating nature of stationary random signals. Nonetheless an attempt to 'visualize' the large eddy has been made using the shot noise decomposition to obtain the magnitude of the eddy's velocity field, and ignoring for now possible phase differences across the jet. The results look very much like the roller eddies reported by various authors.

Acknowledgements. The work described above has been carried out by Mark Glauser, Stewart Leib and Muhammed S. S. Khwaja as a part of their thesis research. This research was initiated under support from the National Science Foundation under Grant No. ENG76-17466 and the Air Force Office of Scientific Research under Contract Nos. F4962078C0047 and F4962080C0053. Work has continued under NSF Grant No. MEA 8316833 and with the support of the NASA trainee program, SJL at NASA/Lewis and MNG at NASA/Ames. These sources of support are gratefully acknowledged.

References

- Baker C. T. H. (1977): *The Numerical Treatment of Integral Equation* (Clarendon, Oxford, New York)
- Bradshaw, P., Ferriss, D. H., Johnson, R. F. (1964): Turbulence in the noise-producing region of a circular jet. *J. Fluid Mech.* **19**, 591
- Cantwell, B. J. (1981): Organized motion in turbulent flow. *Ann. Rev. Fluid Mech.* **13**, 457
- Crow, J. C., Champagne, F. H. (1971): Orderly structure in jet turbulence. *J. Fluid Mech.* **48**, 547
- Davies, P. O. A. L., Barratt, M. J., Fisher, M. J. (1963): The characteristics of turbulence in the mixing region of a round jet. *J. Fluid Mech.* **15**, 337
- Grant, H. L. (1958): The Large Eddies of Turbulent Motion. *J. Fluid Mech.* **4**, 149
- Hussain, A. K. M. F. (1981): "Coherent Structures and Studies of Perturbed and Unperturbed Jets". *Proc. of Int. Conf. on Role of Coherent Structures in Modelling Turbulence and Mixing*, U. Politechnic, Madrid
- Laurence, J. C. (1956): Intensity, scale and spectra of turbulence in mixing region of free subsonic jet. NACA Report No. 1292
- Leib, S. J., Glauser, M. N., George, W. K. (1984): An application of Lumley's orthogonal decomposition to the axisymmetric turbulent jet mixing layer. Presented at 9th Rolla Symposium.
- Lumley, J. L. (1967): "The Structure of Inhomogeneous Turbulent Flows," in *Atm. Turb. and Radio Wave. Prop.*, ed by A. M. Yaglom and V. I. Tatarsky, (Nauka, Moscow) pp. 166-178
- Lumley, J. L. (1981): "Coherent structures in turbulence". *Trans. and Turb.*, Academic Press. edited by R. E. Meyer NY 215-241
- Townsend, A. A. (1956): *The Structure of Turbulent Shear Flow* (Cambridge University Press)
- Townsend, A. A. (1976) 2nd ed: *The Structure of Turbulent Shear Flow* (Cambridge University Press)